JOURNAL OF MATERIALS SCIENCE **36** (2001) 4273–4278

Static recrystallization kinetics of 304 stainless steels

SANG-HYUN CHO
Department of Metallurgical Engineering, McGill University, 3610 University Street, Montreal, Canada H3A 2B2

YEON-CHUL YOO
Department of Materials Science and Engineering, Inha University, 253 Yonghyun-Dong, Nam-Ku, Inchon 402-751, Korea
E-mail: ycyoo@inha.ac.Kr

Static restoration mechanism during hot interrupted deformation of 304 stainless steel was studied in the temperature range from 900 to 1100°C, various strain rate from 0.05 to 5/sec and pass strain of 0.25–3 times peak strain. It was clarified that the static recrystallization was happened after 3–10 seconds at first deformation. The static restoration was depended on the pass strain, deformation temperature and strain rate and fractional softening (FS) values increased with increasing strain rate, deformation temperature and pass strain. Recystallization kinetics was explained with Avrami equation and Avrami constant was 1.113. This value was independent of deformation variables significantly. The time of 5, 50, 95% recrystallization was evaluated using such equations: $t_{0.05} = 2.9 \times 10^{-12}$ $\varepsilon^{-1.17}\dot{\varepsilon}^{-0.94} D \exp(222000\ \text{J/mol}/RT)$, $t_{0.5} = 2.0 \times 10^{-10}$ $\varepsilon^{-1.56}\dot{\varepsilon}^{-0.81} D \exp(197000\ \text{J/mol}/RT)$, $t_{0.95} = 1.9 \times 10^{-8}\varepsilon^{-1.63}\dot{\varepsilon}^{-0.76} D \exp(173000\ \text{J/mol}/RT)$. The predicted values by use of upper equations had a good agreement with a measurement.

1. Introduction

Hot rolling normally involves multi pass deformation process that repeats dynamic and static states. Most studies about hot workability have, however focused on dynamic states like predicting the deformation resistance, microstructure evolution or stress-strain curve modeling and neglected on the static states [1–3]. The materials have to have a static restoration after deformation, because of thermodynamically unstable. Then, static restoration kinetics is depended on the given temperature and strain and recovery, recrystallization or metadynamic recrystallization processes control this kinetics [4, 5]. Such a static restoration is one of the most important processes to determine the material's properties during multipass deformation, which repeated the dynamic and static states like hot rolling. The precise prediction of time for softening and kinetics is therefore related with increment of material's mechanical properties. As austenitic stainless steels especially have higher critical strain for dynamic recrystallization (DRX) and deformation resistance than those of normal carbon steels, thus it's more effective to use the static softening for improving the mechanical properties than dynamic softening.

The static restoration kinetics depends on deformation conditions like pass strain, strain rate, temperature and initial grain size etc., and the softening fraction according to time changes normally shows sigmoid shape and can be expressed by Avrami equation [6]. The studies on static softening about normal carbon steel are preferentially reported that the thermodynamic and microstructure effects on kinetics, the various deformation variables effects and the time for 50% softening ($t_{0.5}$) [7–10]. However there're only few studies about stainless steel. In this study, we investigated the effects of temperature, strain rate and pass strain on static softening and explained by Avrami equation. The times for 5, 50 and 95% softening were also determined.

2. Experimental procedure

AISI 304 stainless steel of nominal composition Fe-18.25 wt% Cr-8.16 wt% Ni was produced by vacuum induction melting (Table I) and hot rolled as 20 mm thickness. Torsion test specimens with a gauge section of 20 mm length and 5 mm radius were machined from the hot rolled steels. Interrupted torsion tests were then conducted over the temperature range 1100–900°C, strain rate range 5.0×10^{-2}–5.0×10^{0}/sec, interpass time range 0.5–100 seconds, and pass strain range 1/4–3 times the peak strain (Table II). This was done so as to evaluate the effects of the deformation variables on metadynamic softening.

The measured torque Γ and twist θ were converted to von Mises effective stress (σ) and strain (ε) using the following equations [11]:

$$\sigma = \frac{3.3\sqrt{3}\Gamma}{2\pi R^3}, \qquad \varepsilon = \frac{\theta R}{\sqrt{3}L} \tag{1}$$

TABLE I The chemical composition of 304 stainless steel used, wt%

C	Si	Mn	P	Cr	Ni	Cu
0.045	0.45	1.03	0.025	18.21	8.16	0.16

TABLE II Summary of multistage deformation process

Interrupted Deformation	Temperature (°C)	900, 1000, 1100
	$\dot{\varepsilon}$ (/sec)	0.05 0.5 5
	t_I (sec)	0.5, 1, 3, 10, 50, 100
	Pass strain	$\varepsilon_I = 0.25,\ 0.5,\ 1$ and $3\varepsilon_p$

Here, R and L are the gauge radius and length of the specimen, respectively. In order to determine the time for 50% recrystallization, the value of the torque associated with yielding was defined using a 0.2% offset method in the multiple twisted torsion tests. The amount of static softening during each pass can be calculated as follows by the following equation:

$$\mathrm{FS} = \frac{\sigma_m - \sigma_{y1}}{\sigma_m - \sigma_{y2}} \quad (2)$$

where σ_m is the maximum stress at the end of the first pass, σ_{y1} is the yield stress at the first pass and σ_{y2} is the yield stress at second pass. Note that Li *et al*. found that the fractional softening calculated using an offset of 0.2% is approximately the same as that determined from the mean flow stress method [12]. By contrast, the softening measured using the present 2% offset approach is consistently lower than that calculated using either the 0.2% offset or the mean flow stress technique. Thus they concluded that the 2% offset method is particularly well suited for following the progress of recrystallization alone (while neglecting the softening attributable to recovery). In practice, the 2% offset method avoids the noise that sometimes appears in the early part of experimental high temperature flow curves. In this way, it makes the calculations of fractional softening more relaible.

3. Results

3.1. Hot interrupted flow curves

Fig. 1 shows the flow curve of 304 stainless steel obtained for a temperature of 1000°C, a constant strain rate of 0.5/sec and interpass time of 0.5–100 seconds. And a pass strain was a half of peak strain at that time,

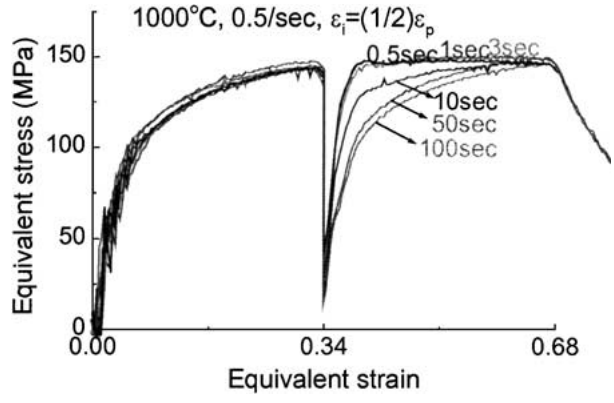

Figure 1 Double-twist flow curves obtained from interrupted torsion tests.

because of excluding of dynamic recrystallization. As it is known, the critical strain for dynamic recrystallization is normally 0.6–0.8 times of peak strain and once, the given strain is over the critical strain, dynamic recrystallization will be dominant softening mechanism. As the interruption time increased, the shapes of second flow curves were different. It's known that the static softening might happen after 3 seconds interruption time from this Fig. 1. After 10 seconds interruption time, the second flow curve indicates that some amount of softening are happened with similar slope of the first flow curve's, rather than work hardening. It exhibits that grain size can be decreased by recrystallization and many amounts of dislocations can also be annihilated. It can be find the same appearance at the different deformation variables like temperature and strain rate; as the strain rate or temperature increases, the flow curve is similar to the first one. Although, the examination of flow curves can't indicate the precise recrystallization starting time or amount of softening, but can show what the outbreak of softening is impossible to state. The effects of pass strain, temperature and interruption time on the next deformation can be presumed from the interrupted flow curves like Fig. 1.

3.2. Fractional softening, FS

Figs 2–4 show the fractional softening as a function of time in each deformation variables calculated by Equation 2. All softening curves present the typical 's'

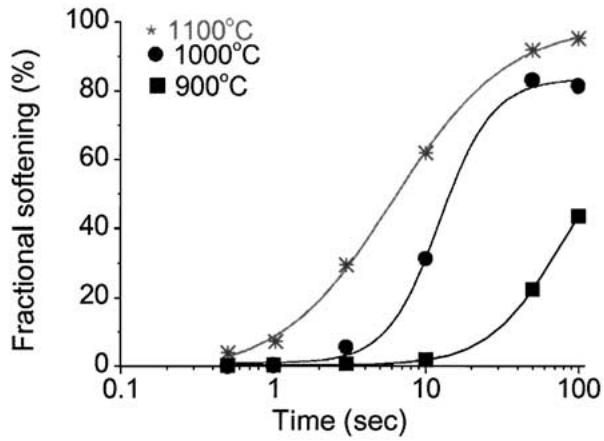

Figure 2 Effect of temperature on the rate of softening.

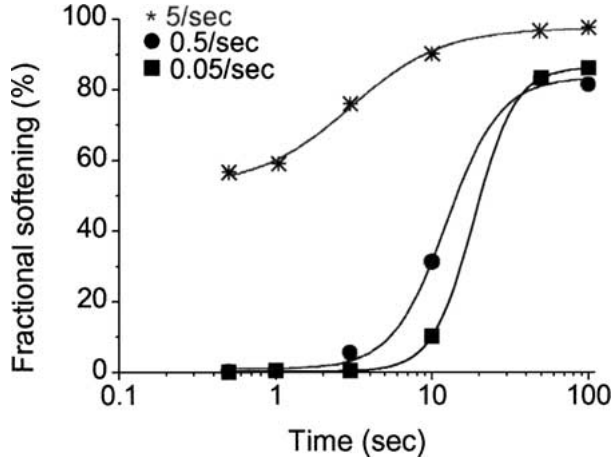

Figure 3 Effect of strain rate on the rate of softening.

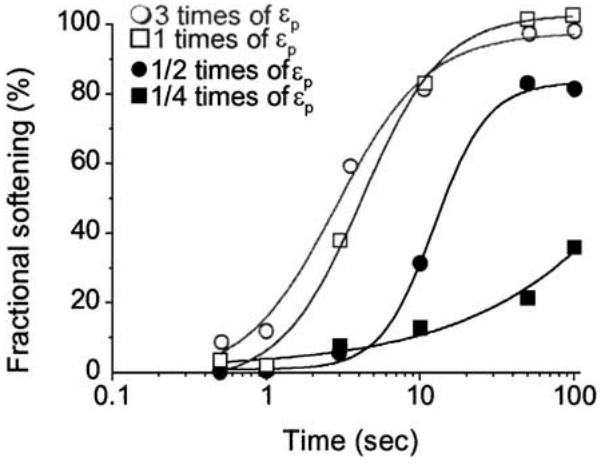

Figure 4 Effect of pass strain on the rate of softening.

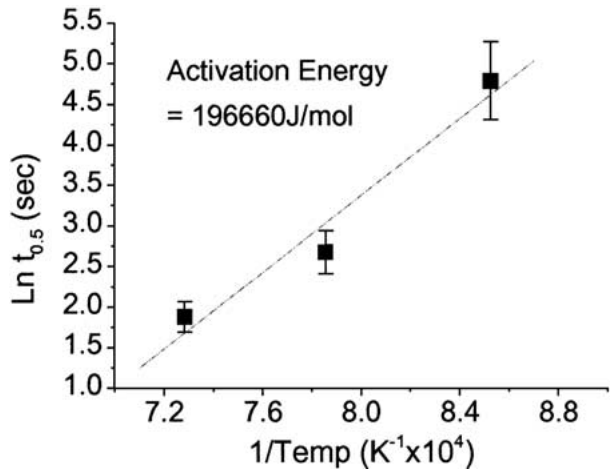

Figure 6 Plot of $t_{0.5}$ against the reciprocal of the temperature.

shape and it means that the static softening depends on time. Fig. 2 exhibits the effect of deformation temperature; the softening kinetics increases, as the temperature increases from 900 to 1000°C, because recrystallized grain boundary's mobility increases, as deformation temperature increases. Fig. 3 presents the effect of strain rate; as the strain rate increases from 0.05 to 5/sec, the much amounts of softening are happened. The effect of pass strain is also presented in Fig. 4; the time for 50% recrystallization decreases about 100 seconds, as the pass strain increases from 1/4 to 3 times of peak strain.

3.3. Recrystallization kinetics

Figs 2–4 display the typical sigmoid shape and the such a recrystallization kinetics can be described by the usual Avrami equation:

$$X_{\mathrm{SRX}} = 1 - \exp\left[- 0.693\left(\frac{t}{t_{50\text{ for SRX}}}\right)^n\right] \qquad (3)$$

Here,

$$t_{50\text{ for SRX}} = A\dot{\varepsilon}^p \varepsilon^q D_0 \exp\left(\frac{Q}{RT}\right) \qquad (4)$$

Where n is Avrami time constant, $t_{50\text{ for SRX}}$ is the time for 50% recrystallization, $\dot{\varepsilon}$ is strain rate, ε is pass strain, D_0 is initial grain size and A, p and q are constants.

Fig. 5 present ln(ln(1/(1 − X)) as a function of ln(time) to calculate the Avrami constant, n. All the deformation conditions like deformation temperature, strain rate and pass strain are showed at the same time in this figure and they shows almost same slope. The Avrami constant can be determined as 1.02 and it is reported that these values of most materials which happened static recrystallization are 1–2 and the deformation variables normally make no difference at that time [13]. Some studies however report this n value can be affected by temperature and initial grain size; as the grain size increases or temperature decreases, n value decreases from 2 to 1 [14]. If grain size is especially very fine less than 50 μm, the n value is going to be fixed as 1 having no connection with deformation variables or chemical composition [15]. However, these are still not well researched about different value of n.

Fig. 6 shows the relationship between $t_{0.5}$ and temperature to determine the activation energy for static softening. The activation energy can be calculated as 197 kJ/mol and this value is very smaller than that of dynamic softening (380 kJ/mol) [16]. It means that the dependency of temperature for static softening is lower than that of dynamic softening.

The time for static softening related with all variables like temperature, pass strain and strain rate, therefore it is needed for the relations; $t_{0.5} \propto \dot{\varepsilon}^p$, $\propto \varepsilon^q$, to analyze $t_{0.5}$. In this experiment, the value of p and q are determined as −1.56 and −0.81. Fig. 7 predicts the time change according to the amount of softening and

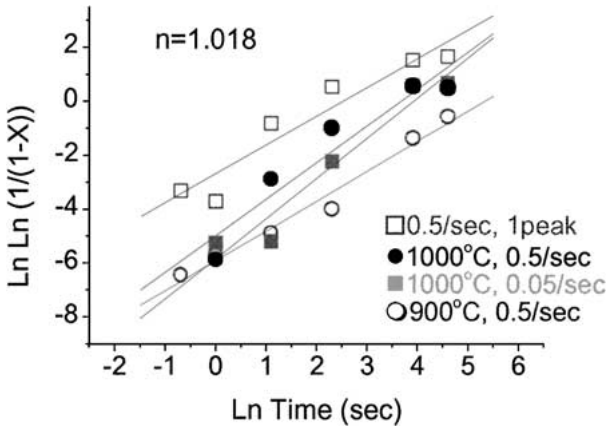

Figure 5 Dependence of ln ln[1/(1 − X)] on ln t under different conditions of pass strain, temperature and strain rate.

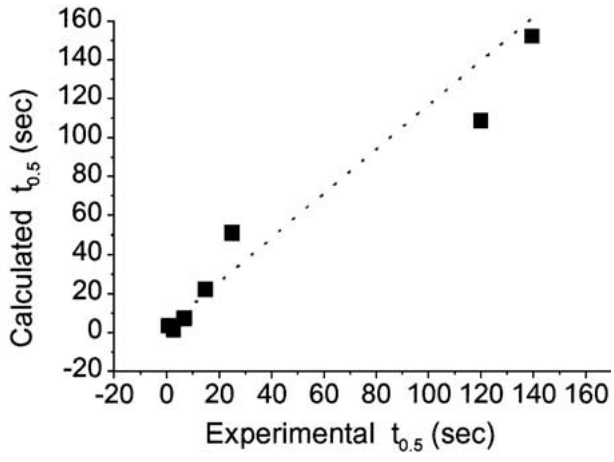

Figure 7 Comparison of experimental and calculated $t_{0.5}$.

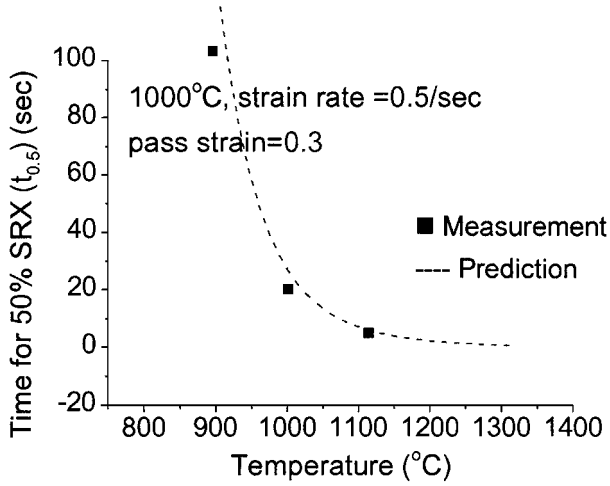

Figure 8 Comparison between the measured and predicted recrystallization values for various deformation temperature.

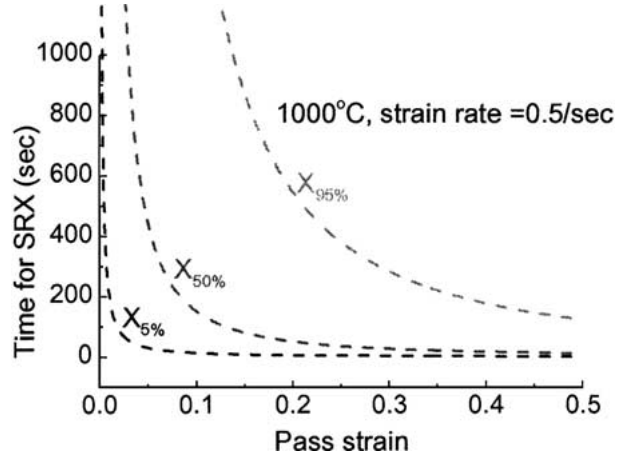

Figure 9 Prediction of time for 5, 50, 95% softening with varying pass strain.

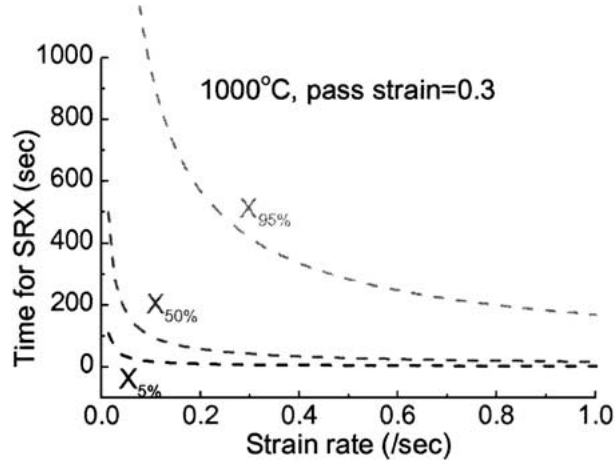

Figure 10 Prediction of time for 5, 50, 95% softening with varying strain rate.

the calculated fraction values are well matched with the experimental values. Fig. 8 shows the $t_{0.5}$ as a softening function according to temperature changes. It is found that the time for 50% recrystallization decreases up to 10 seconds, as temperature increases. The starting and ending point can be easily distinguished in softening curves by adding the straight lines but it is also known by determining the time for 5, 50, 95% distinctly like Equation 4. The $t_{0.05}$ and $t_{0.95}$ can be also determined. The relationship between $t_{0.05}$ and deformation variables could be expressed by the following power relation; $t_{0.05} \propto \varepsilon^{-1.17}$. Also, the dependencies of and $t_{0.95}$ on temperature, strain rate and pass strain were obtained by the above method and the $t_{0.05}$, $t_{0.5}$ and $t_{0.95}$ were shown at Table III. The calculated time for 5, 50, 95% softening also compared to experimental values in Table IV. There were a little difference at the condition of high strain rate and low temperature (high Zener-Hollomon parameter value [17]) but the calculated values were well matched with the experimental values at most conditions.

TABLE III Strain, strain rate and temperature dependencies of time for 5, 50 and 95% recrystallization for 304 stainless steel

Conditions	Equations
$X_{5\%}$	$t_{0.05} = 2.9 \times 10^{-12} \varepsilon^{-1.17} \dot{\varepsilon}^{-0.94}\ D \exp(222000\,\mathrm{J/mol}/RT)$
$X_{50\%}$	$t_{0.5} = 2.0 \times 10^{-10} \varepsilon^{-.156} \dot{\varepsilon}^{-0.81}\ D \exp(197000\,\mathrm{J/mol}/RT)$
$X_{95\%}$	$t_{0.95} = 1.9 \times 10^{-8} \varepsilon^{-1.63} \dot{\varepsilon}^{-0.76}\ D \exp(173000\,\mathrm{J/mol}/RT)$

Figs 9–11 presented the time for whole softening fraction in each deformation variables based on upper equations (Table III). Fig. 9 indicated the effect of pass strain on static softening at the condition of 1100°C and 0.5/sec; all the time for starting (5%), 50% and ending (95%) point were decreased exponentially, as the pass strain increased. Fig. 10 showed the effect of strain rate at 1100°C and 1/2 times of peak strain and the effect of strain rate was presented in Fig. 11 at 0.5/sec and 1/2

TABLE IV Comparison between experimental and calculated recrystallization time

			Recrystallization time (s)			Recrystallization time (s)		
Temp. (K)	ε	$\dot{\varepsilon}$ (/sec)	$t_{0.05}$	$t_{0.5}$	$t_{0.95}$	$t_{0.05}{}^{*}$	$t_{0.5}{}^{*}$	$t_{0.95}{}^{*}$
1273	0.34	0.05	8	25	921	12	51	1065
1273	0.34	0.5	3	15	300	2	22	230
1273	0.34	5	0.1	0.5	21	0.2	3	40
1273	0.17	0.5	6	140	900	5	152	713
1273	0.68	0.5	1	7	28	1	7	74
1273	2.04	0.5	0.5	2	20	0.3	1	12
1373	0.34	0.5	0.7	7	82	0.6	7	70
1173	0.34	0.5	18	120	1000	19	109	928

$t_{0.05}$, $t_{0.5}$, $t_{0.95}$: experimental.
$t_{0.05}{}^{*}$, $t_{0.5}{}^{*}$, $t_{0.95}{}^{*}$: calculated.

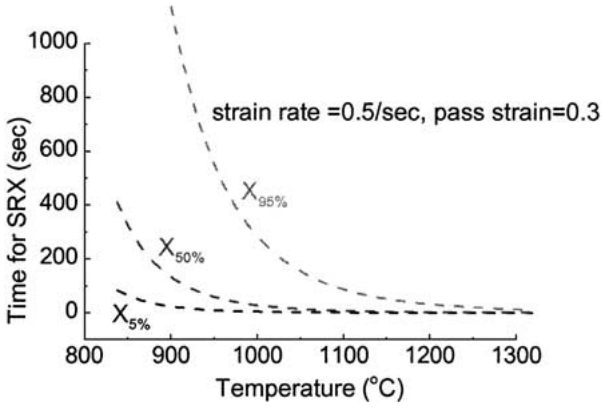

Figure 11 Prediction of time for 5, 50, 95% softening with varying temperature.

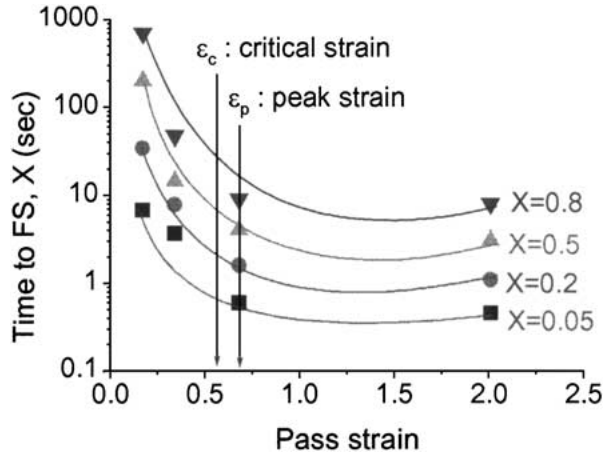

Figure 12 Pass strain dependence of the time for 5 □ □ 80% softening.

times of peak strain. It was confirmed that the time for a certain fraction was decreased, as the strain rate and temperature decreased in each figure but there was little difference, if the deformation temperature increased above 1100°C.

4. Discussion

The amount of softening can be approximately predicted in interrupted flow curve like Fig. 1. The shape of second curve will be different according to the interruption time; if the interpass time is too short, the interrupted flow curve will be same with continuous curve, however the interruption time is longer than 10 seconds, the second curve including some dislocations will be same with the first work hardening curve, because these time is enough to release the accumulated dislocation at the high temperature. During interruption time, static recovery and static recrystallization can be happened, and these two mechanisms are raised competitively by driving force obtained from deformation energy during first deformation. Static recovery has normally no incubation time and the recovered grain rearranges to reduced dislocation density. The subgrain boundaries changes to be sharp and these subgrain boundaries diminishes finally and a nucleation of new grain which has no dislocation is created. Theses nucleus are growing during static recrystallization and make the material soft.

As shown in Figs 2–4, the primary softening kinetics are very slow. The first stage's kinetics depends on the static recovery or the nucleation rate for new grain etc. in this time. Some studies report the softening fraction of recrystallization is 20–30% [17] but we apply the stating point of recrystallization as the time for 5% recrystallization in this experiment (Fig. 8). Generally, the fractional softening, FS can be divided by three different regions. If only dynamic recovery has occurred, the low degree of FS (<30%) is mainly due to the static recovery. High degree of FS ($30 < FS < 100\%$) is usually associated with the partial to complete static recrystallization. The 100% FS indicates the perfect recrystallization and grain growth [14, 15]. If the softening curves of Figs 1 and 2–4 are therefore assembled, it might be good that the time for 5% softening is determined as starting point of recrystallization.

It can be known that the softening kinetics depends on the various deformation conditions in Figs 2–8 and the dependency of pass strain is again presented in Fig. 12. Fig. 12 shows the time for 5, 20, 50 and 80% softening as a function of pass strain. In Fig. 12, a very small change in the softening kinetics was observed when the pass strain was increased after critical strain for dynamic recrystallization (indicated as arrow). On the other hand, a significant increase in kinetics was observed when the pass strain was raised before the critical strain. These curves indicate that the metadynamic softening was happened during the interpass time, when the pass strain was over the critical strain and also that the effect of pass strain for metadynamic softening was negligible. Metadynamic recrystallization occurs by the continued growth of nuclei formed as a result of the occurrence of dynamic recrystallization during prestraining [14]. This softening can be therefore happened at the material, which has dynamic recrystallization as hot deformation mechanism and also has enough prestrain, over critical strain ($\varepsilon > \varepsilon_c$). Hence the operation of MDRX does not require an incubation time and such a rapid interpass softening can increase the mechanical properties, even though not long pass strain and interpass time, especially for materials with relatively large deformation resistance such as austenitic stainless steel. This is also important to improve the mechanical properties and can make very fine grains during the very short interpass time. Therefore, this fast softening can reduce the interpass time and pass strain, since can accelerate the recrystallization during short interpass time. Also, we can obtain the same results considering the softening kinetics. In Fig. 12, the strain accumulation can be balanced with the strain annihilation after critical strain, because of dynamic recrystallization, and the retained strain, which can be driving force for softening, is going to be constant.

Static recrystallization is one of the thermally activated processes, so the activation energy can be obtained from Fig. 6. Time for 50% softening has a linear relationship with temperature and the slope is Q/R. In case of stainless steel, there is very few studies about static softening kinetics and it is known the activation energy for static softening of 240 kJ/mol in case of microalloyed steel [18].

The softening starting time and the amount of softening can be determined by equations at Table I. Many researchers proposed these types of equations little differently. In this experiment, all process variables were considered and the calculated values by these relations showed good agreement with experiments.

The relationship between the time for softening and temperature in Fig. 8 can also explain the relationship between grain size and static softening. The soaking temperature or reheating velocity etc. normally affect all softening mechanism like dynamic and static states, since the microstructures depends on the reheating temperature history. It can be found that the $t_{0.5}$ is reached at almost 0 second, as the temperature increases in Fig. 8. Because as the temperature increases, the subgrain coarsening ratio also increases and grain size will be bigger finally, the thermally activated dislocation density also increases and the grain boundaries can easily move. Other variables like strain rate, strain can affect the static softening and it's because of change of dislocation density, grain boundary's diffusivity or mobility by changing the deformation conditions.

5. Conclusion

The kinetics of static recrystallization behaviors of austenitic stainless steel during hot deformation was described and changes in softening were analyzed. From the analysis of softening behavior, the following conclusions can be drawn:

It's known that the static softening might took place after 3 seconds during interruption from interrupted flow curves and fractional softening and it depended on process variables like strain, temperature and strain rate. Static recrystallization kinetics can be described by Avrami equation and the Avrami constant was determined as 1.02. The deformation variables normally make no difference at this time.

The time for static softening related with all variables like temperature, pass strain and strain rate and the following power relations could express these relationships.

$$t_{0.05} = 2.9 \times 10^{-12} \varepsilon^{-1.17} \dot{\varepsilon}^{-0.94} \times D \exp(222000\,\text{J/mol}/RT)$$

$$t_{0.5} = 2.0 \times 10^{-10} \varepsilon^{-1.56} \dot{\varepsilon}^{-0.81} \times D \exp(197000\,\text{J/mol}/RT)$$

$$t_{0.95} = 1.9 \times 10^{-8} \varepsilon^{-1.63} \dot{\varepsilon}^{-0.76} \times D \exp(173000\,\text{J/mol}/RT)$$

References

1. S. H. CHO, S. I. KIM and Y. C. YOO, *J. Mater. Sci. Lett.* **16** (1997) 1836.
2. K. N. RAMAKRISHNAM, H. B. MCSHANE, T. SHEPPARD and E. K. LOANNIDIS, *Mater. Sci. Technol.* **8** (1992) 709.
3. C. M. SELLARS, *ibid.* **6** (1990) 1072.
4. R. A. PETKOVIC, M. J. LUTON and J. J. JONAS, *Acta Metall.* **27** (1979) 1633.
5. R. A. PETKOVIC and J. J. JONAS, *ISIJ* **210** (1972) 256.
6. M. AVRAMI, *J. Chem. Phys.* **7** (1939) 1103.
7. D. R. BARRACLOUGH and C. M. SELLARS, *Mater. Sci. Technol.* **13** (1979) 257.
8. L. T. MAVROPOULOS and J. J. JONAS, *Can. Metall. Q.* **27** (1988) 235.
9. M. J. LUTON, R. A. PETKOVIC and J. J. JONAS, *Acta Metall.* **28** (1979) 729.
10. A. LAASRAOUI and J. J. JONAS, *Met. Trans.* **22A** (1991) 151.
11. N. D. RYAN and H. J. MCQUEEN *Can. Metall. Q.* **30** (1991) 113.
12. G. LI, T. M. MACCAGNO, D. Q. BAI and J. J. JONAS, *ISIJ International* **36**(12) (1996) 1479.
13. O. KWON, *ibid.* **32** (1992) 350.
14. C. ROUCOULES, P. D. HODGSON, S. YUE and J. J. JONAS, *Met. Trans. A* **25A** (1994) 389.
15. A. LAASRAOUI and J. J. JONAS, *Met. Trans.* **22A** (1991) 151.
16. S. H. CHO, S. I. KIM and Y. C. YOO, *Metals and Materials*, **4**(4) (1998) 732.
17. H. J. MCQUEEN, W. A. and J. J. JONAS, *Can. J. Phys.* **45** (1967) 1225.
18. A. LAASRAOUI and J. J. JONAS, *Met. Trans.* **22A** (1991) 151.
19. O. KWON and A. J. DEARDO, *Acta Metall. Mater.* **38** (1990) 41.

Received 15 February 2000
and accepted 13 April 2001